Building and Environment 63 (2013) 11–19

Contents lists available at SciVerse ScienceDirect

Building and Environment

journal homepage: www.elsevier.com/locate/buildenv

Modeling control measure effects to reduce indoor transmission of pandemic H1N1 2009 virus

Yi-Hsien Cheng, Chung-Min Liao*

Department of Bioenvironmental Systems Engineering, National Taiwan University, Taipei 10617, Taiwan, ROC

ARTICLE INFO

Article history:
Received 15 October 2012
Received in revised form
29 December 2012
Accepted 17 January 2013

Keywords:
Influenza
Pandemic H1N1 2009
Basic reproduction number
Control measure
Airborne infectious diseases
Indoor air quality

ABSTRACT

The pandemic H1N1 2009 (p-H1N1) spreading worldwide has led to severe morbidity and mortality. This study aimed to quantify the impacts on disease control by applying various control strategies for p-H1N1 in an elementary school indoor setting. Indoor disease transmissibility was explored by a general Wells-Riley equation. To better contain influenza outbreak, a multi-control measure model was developed. A non-extinction branching process was presented to quantify the indoor epidemic probability for seasonal influenza and p-H1N1. The infection risk, quantum generation rate (quanta d^{-1}), basic reproduction number (R_0), generation time (d), and asymptomatic infectious proportion (%) were, respectively, estimated to be 0.020 (95% CI: 0.010–0.043), 494 (140–1292), 3.30 (0.75–11.47), 3.54 (3.15–3.99), and 15 (8–59) for p-H1N1. By implementing all non-engineering interventions, seasonal influenza could be well controlled, whereas for p-H1N1, engineering and non-engineering control measure combinations were effective for complete outbreak containment. Indoor epidemic probability of p-H1N1 increases with increments in R_0 and introductions of infected individual. The proposed control strategies combined with non-engineering and engineering interventions could effectively control p-H1N1 outbreak. A multi-control measure model developed here could be implemented in more complex infectious circumstances. Our study can be incorporated into the relationship among influenza virus, host, and indoor environment for better understanding the complex dynamics of environmental processes and to achieve optimal indoor control measures.

1. Introduction

The pandemic H1N1 2009 (p-H1N1), which first emerged in Mexico in April 2009, had spread worldwide, resulting in more than 16,900 laboratory-confirmed cases and 500–1000 deaths in over 67 countries, by mid-February 2011 [1]. The p-H1N1 virus will probably spread in a spatiotemporal pattern similar to those of previous pandemics but accelerated because of increased air travel [2]. Although WHO had declared that p-H1N1 is now in the post-pandemic period, the authority emphasized much on the necessity of epidemiological and virological monitoring because of its emergence and global spread as well as the potential to circulate as a seasonal virus [3]. Moreover, continuous outbreak investigation and population surveillance would substantially support public health decision making.

Although human populations have been continuously exposed to influenza viruses, there is concern that the possible increased pathogenicity of p-H1N1 virus upon reassortment poses unprecedented challenges for mitigation strategies [4]. The epidemiology of p-H1N1 is different from seasonal influenza epidemics, yet unlike previous pandemics. Initially, most cases were clustered in households and schools, with over 50% of the reported cases in schoolchildren in the 5- to 18-year-old age range. Young people had been disproportionately affected in terms of hospitalizations and deaths compared to seasonal influenza in which complications and mortality were predominantly by the elderly [5].

Viral shedding data capture important messages of the virus–host interaction. Many researches had highlighted that the higher viral shedding level reflected the disease severity or impaired host immunity that require instantaneous attention and aggressive treatment [6]. School-aged children were correlated strongly with longer periods of viral shedding or higher secondary attack rate [2,7,8]. This demonstrated the essentiality in surveillance program as well as mitigation strategies among schoolchildren. For the vast majority of the world's population, pharmaceutical interventions, such as vaccines and antivirals, will not have a significant role in the current pandemic [9].

* Corresponding author. Tel.: +886 2 2363 4512; fax: +886 2 2363 6433.
E-mail address: cmliao@ntu.edu.tw (C.-M. Liao).

0360-1323/$ – see front matter © 2013 Elsevier Ltd. All rights reserved.
http://dx.doi.org/10.1016/j.buildenv.2013.01.014

Therefore, any coordinated public-health effort to reduce the impact of the pandemic must rely largely on the combined effect of non-pharmaceutical interventions, such as school closures, restriction on mass gatherings, increased use of personal protective measures, *e.g.*, face masks, hand hygiene, cough etiquette, and early self-isolation when ill [9]. Fraser et al. [10] proposed a two-efficacy control measure model derived from a von Foerster equation based-criteria to examine the likely success of public control measures in containing outbreaks for SARS, HIV, smallpox, and influenza. Where basic reproduction number (R_0) and asymptomatic infectious proportion (θ) are two key determinants in constructing the critical control curve and to see whether the disease is under control.

Lots of effort had been made to investigate the influenza transmission as well as the disease control indoors [11–14]. The ways to estimate the indoor transmissibility of p-H1N1 and seasonal influenza virus play crucial role in designing effective indoor mitigation strategies. Specifically, the best characterization of influenza transmissibility has been based on R_0, defining as the average number of successful secondary infection cases generated by a typical primary infected case in an entirely susceptible population [15]. R_0 can be estimated from outbreak investigation data to give insight into how underlying transmission dynamics will influence the likely impact of possible interventions.

Evaluating the impact of different indoor control measures on the spread of respiratory diseases has been limited by a lack of detailed data on transmission in indoor settings as well as appropriate statistical methods. Here we analyzed data from a p-H1N1 outbreak in Taiwan regions started in May 2009 and used an elementary school as an indoor setting to investigate how pharmaceutical and non-pharmaceutical interventions affect p-H1N1 transmission. Here we used seasonal influenza as a comparison.

The objectives of this work were to: (1) describe and predict the behavior and the impacts of the p-H1N1, (2) demonstrate the potential outcomes of proposed pharmaceutical and non-pharmaceutical interventions with engineering control measures in elementary school indoor settings, and (3) compare with seasonal influenza to capture the full impact of the p-H1N1 on morbidity. Here we used epidemiological models of influenza to investigate how pharmaceutical and non-pharmaceutical interventions contributing to achieving particular objectives for reducing indoor transmission of emerging p-H1N1.

2. Materials and methods

2.1. Study data

This study analyzed the weekly basis laboratory surveillance data of confirmed influenza infection cases obtained from Centers for Disease Control, Taiwan (Taiwan CDC) by the date of symptom onset in the period 2001–2009. These reanalyzed data were used to compare the infection risks between seasonal influenza (A (H1N1), A (H3N2) and type B) and pandemic H1N1 2009 (p-H1N1). Influenza-like illness (ILI) admission cases were provided by Department of Health, Taiwan (Taiwan DOH), including identified and unidentified influenza patients. ILI surveillance was conducted by sentinel primary care physicians based on integrated clinical and virological surveillance components. According to ICD-10-CM (International Classification of Diseases, Tenth Revision, Clinical Modification), ILI was defined as the occurrence of flu-like illness lasting for at least two days and having at least one systemic symptom: fever ($\geq$38 °C), headache, chills, myalgia, fatique, and at least one respiratory symptom: sore throat, cough, rhinorrhea, hoarseness, and runny or stuffy nose [16,17].

However, not all ILI cases would admit to clinics or hospitals, moreover, among those ILI admission cases, only part of those ILI samples would go through laboratory-based influenza infection confirmation. Therefore, to better examine the national level based infection risk (P) among various (sub)types of influenza in school-aged children, this study extended the positive proportions as to divide ILI positive proportion by admission proportion,

$$P = \frac{\text{ILI positive proportion}}{\text{Admission proportion}}, \tag{1}$$

where the admission proportion was school-aged children-based (5–14 yr), defined as the ratio of ILI admission cases to mid-year population numbers can be treated as an adjust factor to scale up the positive proportion to national level.

2.2. Indoor air transmission model

Wells-Riley mathematical equation was extensively applied to describe the airborne disease transmission and to assess the potential infection risks in an enclosed indoor environment. Epidemic characterizations of P can be calculated by the Wells-Riley mathematical equation [18],

$$P = \frac{D}{S} = 1 - \exp\left\{\frac{-iqpt}{Q}\left\{1 - \frac{V}{Qt}\left[1 - \exp\left(\frac{-Qt}{V}\right)\right]\right\}\right\}, \tag{2}$$

where D is the number of confirmed infected cases, S is the number of susceptible individuals, i is the number of infectors, q is the quantum generation rate by an infectious infector (quanta h^{-1}), p is the breathing rate per person ($m^3\ h^{-1}$), t is the total exposure time (h), Q is the fresh air supply rate that can remove infectious aerosol particles ($m^3\ h^{-1}$), and V is the volume of the ventilated space (m^3).

Eq. (2) can be rewritten to estimate the quantum generation rate, q,

$$q = \frac{-Q\ln(1-P)}{ipt\left\{1 - \frac{V}{Qt}\left[1 - \exp\left(\frac{-Qt}{V}\right)\right]\right\}}. \tag{3}$$

By incorporating the initial respiratory infection conditions of $i = 1$ and $S = n - 1$ into Eq. (2) where n stands for the number of total population indoors, R_0 can be estimated accordingly [18],

$$R_0 = \left(n-1\right)\left\{1 - \exp\left\{\frac{-qpt}{Q}\left[1 - \frac{V}{Qt}\left(1 - \exp\left(\frac{-Qt}{V}\right)\right)\right]\right\}\right\}. \tag{4}$$

This study took into account an elementary school setting to assess the indoor transmission risks and the severity of influenza infection among schoolchildren.

2.3. Key epidemiological determinants estimation

Generally, asymptomatic infectious proportion (θ) was used to estimate the proportion of transmission occurring prior onset of symptoms. Thus the potential of public health control measures based on symptomatic population can be estimated [10]. By definition, θ can be calculated as [10],

$$\theta = \frac{\text{Incubation period} - \text{Latent period}}{\text{Mean duration of viral shedding}}, \tag{5}$$

where incubation period is the interval from the point of infection to the appearance of symptoms and latent period is the interval from the point of infection to the infectious state beginning.

On the other hand, the time interval between infection of a primary case and infection of a secondary case caused by the primary case can be characterized by the generation time (T_g) [10]. To estimate T_g, previous data were used. Specifically, Cowling et al. [7] provided the data related to the viral shedding levels of seasonal and pandemic influenza A varied with days post illness onset. On the other hand, Carrat et al. [19] provided the viral shedding dynamic data among various (sub)types of seasonal influenza.

Firstly, this study shifted the viral shedding dynamic data of p-H1N1 from day 0 post illness onset to day 2 post infection. Based on the similar characteristics of viral shedding and clinical illness in p-H1N1 as that observed in seasonal influenza A viruses [7], Viral shedding of days 0 and 1 post infection for p-H1N1 were estimated, respectively, through the data of days 0 and 1 post infection of seasonal influenza A (H1N1) virus [19] by multiplying the area under the curve (AUC) ratio of $AUC_p/AUC_s = 1.20$ where AUC_p is the AUC of viral shedding dynamic of p-H1N1 and AUC_s is the AUC of viral shedding dynamic of seasonal influenza.

In this study, we developed a general form of multiple efficacy control measure model as (see Appendix 1 in Supplementary materials)

$$R_0\left\{\left[\prod_{j=1}^{N}(1-\varepsilon_j)\right]\sum_{p=0}^{N}\left\{\frac{\theta}{p-(p-1)\theta}\sum_{\sum L_j=p, L_j\in\{0,1\}}\left[\left(\frac{\varepsilon_1}{1-\varepsilon_1}\right)^{L_1}\times\left(\frac{\varepsilon_2}{1-\varepsilon_2}\right)^{L_2}\cdots\left(\frac{\varepsilon_N}{1-\varepsilon_N}\right)^{L_N}\right]\right\}\right\}=1, \quad (8)$$

where ε_j represents the control measure efficacy and p and L are the integers.

In the present study, we used a four-efficacy based equation to be the indoor control measure model as (see Appendix 1 in Supplementary materials)

$$R_0\left\{\begin{array}{l}(1-\varepsilon_1)(1-\varepsilon_2)(1-\varepsilon_3)(1-\varepsilon_4)+[\varepsilon_1(1-\varepsilon_2)(1-\varepsilon_3)(1-\varepsilon_4)+\\ \varepsilon_2(1-\varepsilon_1)(1-\varepsilon_3)(1-\varepsilon_4)+\varepsilon_3(1-\varepsilon_1)(1-\varepsilon_2)(1-\varepsilon_4)+\varepsilon_4(1-\varepsilon_1)(1-\varepsilon_2)(1-\varepsilon_3)]\theta+\\ \left[\begin{array}{l}\varepsilon_1\varepsilon_2(1-\varepsilon_3)(1-\varepsilon_4)+\varepsilon_1\varepsilon_3(1-\varepsilon_2)(1-\varepsilon_4)+\varepsilon_1\varepsilon_4(1-\varepsilon_2)(1-\varepsilon_3)+\\ \varepsilon_2\varepsilon_3(1-\varepsilon_1)(1-\varepsilon_4)+\varepsilon_2\varepsilon_4(1-\varepsilon_1)(1-\varepsilon_3)+\varepsilon_3\varepsilon_4(1-\varepsilon_1)(1-\varepsilon_2)\end{array}\right]\left(\frac{\theta}{2-\theta}\right)+\\ [\varepsilon_1\varepsilon_2\varepsilon_3(1-\varepsilon_4)+\varepsilon_1\varepsilon_2\varepsilon_4(1-\varepsilon_3)+\varepsilon_1\varepsilon_3\varepsilon_4(1-\varepsilon_2)+\varepsilon_2\varepsilon_3\varepsilon_4(1-\varepsilon_1)]\left(\frac{\theta}{3-2\theta}\right)+\\ \varepsilon_1\varepsilon_2\varepsilon_3\varepsilon_4\left(\frac{\theta}{4-3\theta}\right)\end{array}\right\}=1. \quad (9)$$

Both AUC_p and AUC_s can be estimated by integrating the fitted homogeneous Poisson process equation,

$$V(t) = \alpha\mu\exp(-\mu t), \quad (6)$$

where $V(t)$ is the absolute level of viral shedding at time t post infection ($\log TCID_{50}$ mL^{-1} where TCID50 was measured as 50% tissue culture infective dose), α is the fitted AUC constant ($\log TCID_{50}$ mL^{-1} day), and μ is the viral shedding reducing rate (day^{-1}). The T_g could be calculated based on an assumption that infectiousness is proportional to viral shedding [19],

$$T_g = \frac{\int_0^\infty tV(t)dt}{\int_0^\infty V(t)dt}. \quad (7)$$

2.4. General indoor control model

Fraser et al. [10] developed two-efficacy based control measure model. Two critical epidemiological determinants R_0 and θ together with different control efficacies (ε_j) were used to construct the critical control curve [10] where ε_j is defined as the potential to reach expected control effect. Below the curve represents optimal control measure is eventually achieved. The uncontrollable (UC) ratio can be calculated as the ratio of the area above the control curve to the total area obtained by considering both confidence intervals of R_0 and θ. Non-engineering control measures were weighed in this study for seasonal influenza and p-H1N1, whereas in latter both engineering and non-engineering control measures were combined to contain p-H1N1 based on its transmissibility.

Non-engineering public health control strategies were individually or combinatively implemented in estimating the potential of disease containment. The additive control impacts of engineering controls were quantified by R_c and θ, where R_c is the engineering control-based basic reproduction number estimated by combined Wells-Riley equation and competing risk model [20],

$$R_c = (n-1)\left\{1-\exp\left\{\left[\frac{-iqtp(1-\eta_s)}{(ACH_e+\lambda+ACH_r)V}\right]\times[1-\exp(-(ACH_e+\lambda+ACH_r)t)]\right\}\right\}, \quad (10)$$

where η_s is the fractional respiratory protection over a person by surgical mask (SM), ACH_e is the air exchange rate enhanced through further ventilation (EV) (h^{-1}), λ is the inactivation rate of infectious droplet nuclei due to ultraviolet germicidal irradiation (UVGI) (h^{-1}), and ACH_r is the air exchange rate through a recirculated high efficiency particulate air (HEPA) filter (h^{-1}).

2.5. Indoor epidemic probability model

Here a non-extinction branching process was used to describe the infectiousness of p-H1N1 and its fraction of infection within a population indoors (*i.e.*, indoor epidemic probability). Epidemic can be defined as the occurrence of more diseased cases than expected in a given human population and area during a particular period of time. Suppose an organism in the end of its lifetime generates a random number ξ of offspring with probability p_k and ξ has a Poisson distribution with a mean λ for which

$$p_k = \Pr\{\xi = k\} = \frac{\lambda^k e^{-\lambda}}{k!} \quad \text{for } k = 0, 1, \ldots, \quad (11)$$

then the probability generating function (pgf) $\phi(s)$ can be written as [21]

$$\phi(s) = E\left[s^{\xi}\right] = \sum_{k=0}^{\infty} s^k \frac{\lambda^k e^{-\lambda}}{k!} = e^{-\lambda} \sum_{k=0}^{\infty} \frac{(\lambda s)^k}{k!} = e^{-\lambda(1-s)}. \quad (12)$$

while considering the population non-extinction processes with a Poisson distribution, the pgf can be written as [21]

$$1 - u_z = 1 - \sum_{k=0}^{\infty} \frac{\lambda^k e^{-\lambda}}{k!} (u_{z-1})^k = 1 - \phi(u_{z-1}) = 1 - e^{-\lambda(1-s)}, \quad (13)$$

where $u_z = \Pr\{X_z = 0\}$ describes the probability that a population at its zth generation the population size X_z equals 0.

Theoretically, assuming a homogeneous and unstructured population, the total proportion of infected population (I) during the epidemic depends only on R_0 [15],

$$I = 1 - \exp(-R_0 I). \quad (14)$$

We incorporated the concept of non-extinction branching process (Eq. (13)) into Eq. (14) to construct the indoor epidemic probability. Therefore, by giving the mean value of R_0 distribution (R_m) and the infection number in the ventilated enclosure (i), the conditional probability of indoor epidemic as the function of effective reproduction number (R_e) can be written as

$$P(I(R_e)|i; R_m) = 1 - \exp[-i \cdot R_m(R_e - 1)], \quad (15)$$

where $R_e > 1$ that enables disease outbreak.

The overall equations used in present study for estimating specific epidemiologic parameters are summarized in Table S1 (see Supplementary materials). The uncertainty and its impact on the expected risk estimate were quantified by a Monte Carlo (MC) simulation technique. A MC simulation was carried out with 10,000 iterations to assure the stability of those pdfs and generate 2.5- and 97.5-percentiles as the 95% confidence interval (CI) for all fitted models. The Crystal Ball® software (Version 2000.2, Decisioneering, Inc., Denver, Colorado, USA) was employed to implement the MC simulation.

3. Results

3.1. Indoor transmission parameter estimates

Fig. 1 shows the epidemiology curves of confirmed case in weekly basis in the period 2001–2009 for seasonal influenza A (H1N1), A (H3N2), type B and p-H1N1, respectively. Among the epidemiology curves, p-H1N1 had the most severe incidences in 2009 with the first confirmed case appeared at the end of May and disease outbreak began in late June. The probability distributions of infection risk were estimated based on the epidemic curves. The lognormal (LN) distributions were found to be best describing the infection risk (P) with results 0.0094 (95% CI: 0.0021–0.0391), 0.0068 (0.0017–0.0268), 0.0067 (0.0011–0.0431), and 0.0203 (0.0096–0.0429), respectively, for A (H1N1), A (H3N2), type B, and p-H1N1.

The indoor transmission parameters of quantum generation rate (q) and basic reproduction number (R_0) could be estimated by the Wells-Riley mathematical equation based on an elementary school setting (see Appendix 2 in Supplementary materials) through estimated infection risks (see Table S2 in Supplementary materials). The results show that q estimates were 222 (95% CI: 40–1124), 162 (31–749), 161 (21–1136), and 494 (140–1292) quanta d^{-1} for A (H1N1), A (H3N2), type B and p-H1N1, respectively. On the other hand, p-H1N1 had the largest R_0 estimate of 3.30 (95% CI: 0.75–11.47) followed by A (H1N1) of 1.54 (0.22–8.88) and A (H3N2) and type B of 1.11 (0.18–6.20) and 1.11 (0.12–8.52), respectively.

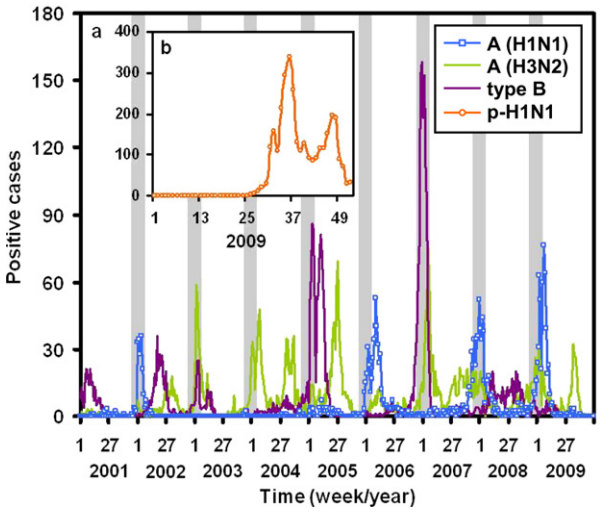

Fig. 1. Weekly-basis epidemiology curves of laboratory confirmed influenza cases in the period 2001–2009 for (a) seasonal influenza A (H1N1) (blue), A (H3N2) (green), and type B (purple) and (b) pandemic H1N1 2009 (p-H1N1) (orange). (For interpretation of the references to color in this figure legend, the reader is referred to the web version of this article.)

3.2. Epidemiological determinant estimates

Asymptomatic infectious proportions were estimated based on the published epidemiological data of incubation period, latent period and infectious period (*i.e.*, mean duration of viral shedding) followed by Eq. (5) (see Table S3 in Supplementary materials). Here the mean incubation and latent periods of 3 and 2 day were used, respectively. Thus, the asymptomatic infectious proportions could be estimated accordingly to be 27 (95% CI: 18–58), 22 (19–27), 19 (17–22), and 15 (8–59) %, respectively, for A (H1N1), A (H3N2), type B and p-H1N1.

Fig. 2 shows the reconstructed viral shedding dynamics for seasonal influenza and p-H1N1, describing well by the homogeneous Poisson processes. Results indicated that for seasonal influenza, the AUC constant (α) and the viral shedding reducing rate (μ) were estimated to be 10.67 $\log TCID_{50}$ mL^{-1} day and 0.29 day^{-1}, respectively ($r^2 = 0.92$, $p < 0.001$) (Fig. 2a), whereas for p-H1N1, α and μ were estimated to be 12.50 $\log TCID_{50}$ mL^{-1} day and 0.34 day^{-1}, respectively ($r^2 = 0.95$, $p < 0.001$) (Fig. 2b). Fig. 3 shows that a 4-parameter lognormal fitting curve could well describe the viral shedding dynamic data.

Epidemiological determinant of generation time T_g could then be estimated by integrating the fitted lognormal viral shedding curve. The estimated T_g were 3.16 (95% CI: 2.84–3.52), 4.14 (3.82–4.50), and 3.62 (3.52–3.73) day, respectively, for A (H1N1), A (H3N2) and type B, whereas in p-H1N1, the estimated T_g was 3.54 (3.15–3.99) day. Table 1 summarizes the estimated epidemiological parameters of P, q, R_0, T_g, and θ for seasonal influenza and p-H1N1.

3.3. Impact of indoor control measures

Given the estimated R_0, θ, and various control efficacies (ε_j), the critical control curve can be constructed (Table 1, Fig. 4). To achieve optimal containment of influenza outbreak, all the maximum control efficacies of non-engineering control strategies were applied

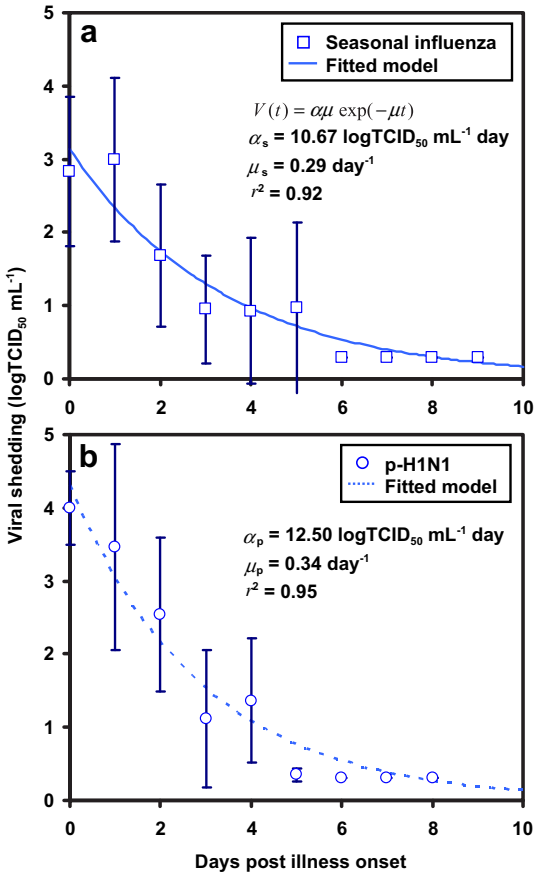

Fig. 2. Homogeneous Poisson process describing the viral load dynamic data for (a) seasonal influenza and (b) p-H1N1. Square and circle represent the viral load data of seasonal influenza and p-H1N1, respectively. The solid and dashed lines show the fitted homogeneous Poisson process for seasonal influenza and p-H1N1, respectively.

including isolation or school closure (ε_i = 100%), pandemic vaccination (ε_{vp} = 62%), seasonal influenza vaccination (ε_{vs} = 57%), surgical mask (ε_{sm} = 58–85%), and hand washing (ε_h = 45%). The potential control measure combinations used in the present control measure model can be categorized into 6 combinations of C1 (ε_i), C2 ($\varepsilon_i + \varepsilon_{sm}$), C3 ($\varepsilon_i + \varepsilon_{vp} + \varepsilon_{sm}$), C4 ($\varepsilon_i + \varepsilon_{vs} + \varepsilon_{sm}$), C5 ($\varepsilon_i + \varepsilon_{vp} + \varepsilon_{sm} + \varepsilon_h$), and C6 ($\varepsilon_i + \varepsilon_{vs} + \varepsilon_{sm} + \varepsilon_h$) (see Appendix 3 and Table S4 in Supplementary materials). The calculated uncontrollable ratios of potential combinations C1–C6 were also presented for seasonal influenza and p-H1N1 (see Table S5 in Supplementary materials).

When control measure C1 was implemented, the calculated uncontrollable ratio of influenza A (H1N1), A (H3N2) and type B were 68.76%, 30.03%, and 40.04%, respectively, whereas 70.50% was estimated for p-H1N1 (Fig. 4 and Table S5 in Supplementary materials). The potentials of other control measures with various combinations (C2, C3, C4, and C6) reveal that seasonal influenza could be well controlled (Fig. 4 and Table S5 in Supplementary materials). However, as for p-H1N1, even though four control strategies (C5) were implemented, the uncontrollable ratio was still higher than 40% (Fig. 4 and Table S5 in Supplementary materials).

To effectively control the outbreak of p-H1N1, we implemented four engineering control measures (see Table S6 in Supplementary materials) together with four non-engineering control measure combinations (C1, C2, C3, and C5) to refine the R_0 distributions of p-H1N1 (*i.e.*, R_c). Amongst these control measure combinations, EV was considered variously within the range 4–12 ACH as to approach the feasible indoor building ventilations. Fig. 5 gives the potential of outbreak containment by applying both non-engineering controls and engineering controls in the combination order as enhanced ventilation, surgical masking, UVGI, and HEPA filter.

The outbreak containment efficiency showed significant improvement of 60 and 71% given EV increased from 4 to 8 and 12 ACH, respectively while only school closure (C1) was implemented (Fig. 5). On the other hand, the more non-engineering control measures being employed (C1 – C5), the lower uncontrollable ratio can be approached (decreasing from 80.54 to 52.02% given EV = 4ACH). Furthermore, while considering lower EV of 4 ACH, wearing surgical mask and turning on UVGI together with C1, the p-H1N1 outbreak was unlikely to occur in a classroom, *e.g.*, the uncontrollable ratio was 7.19%, whereas C3 or C5+4ACH + SM + UVGI showed complete containment. In this study, UVGI can either be substituted with HEPA filter since both interventions display similar equivalent air exchange rate or be employed together depending on the disease outbreak potential.

3.4. Indoor epidemic probability

Fig. 6 shows the probability of an outbreak of seasonal influenza and p-H1N1 in a susceptible population for a range of values of R, approximated by the probability of non-extinction of a branching process in which the number of secondary cases is given by a log-normal distribution with a median R_0 after the introduction of a single, 5, 10, and 50 infectious cases. Generally, the probability of an outbreak from a single introduction increases with R, reaching about 80% for A (H1N1) (Fig. 6a), 67% for A (H3N2) and B (Fig. 6b, c), and 96% for p-H1N1 (Fig. 6d), respectively, for $R = 2$. The probability of an epidemic increases rapidly when there are multiple introductions (Fig. 6a–d).

For p-H1N1, epidemic spread is highly likely when R exceeding 1.5 and there are as few as 5 introductions of the infection into a susceptible population (Fig. 6d). Our results also indicate that, if repeated introduction of seasonal influenza cases into a population failed to result in ongoing transmission, it would be an indication that control measures have effectively reduced R to levels nearly less than 1 (Fig. 6a–c).

4. Discussion

4.1. Indoor disease transmission and control measure model

Parameter q reveals the pathogen infectivity as well as the infectious source strength. Our q estimates were 9 (95% CI: 2–47), 7 (1–31), 7 (1–47), and 21 (6–54) quanta h^{-1}, respectively, for A (H1N1), A (H3N2), type B, and p-H1N1 that fell within the ranges of 34–69, 31–157, and 15–128 quanta h^{-1}, indicating that super-spreaders may not exist in the classroom [18,22,23]. Different indoor settings and calculation methods would result in different q estimates. Based on our q estimation process, it is unlikely to identify whether a super-spreader may exist that may be identified by the follow-up epidemiological and virological monitoring.

In our study, the estimates of R_0 and θ dominate the prioritized recommendations of indoor control strategies. Our R_0 estimate was 3.30 (95% CI: 0.75–11.47) for p-H1N1, whereas for A (H1N1), A (H3N2), type B, the R_0 were estimated to be 1.54 (0.22–8.88), 1.11 (0.18–6.20), and 1.11 (0.12–8.52), respectively. Compared with published literature, our median R_0 estimates for both p-H1N1 and seasonal influenza fell within the published ranges of 1.5–16.5 [18], 5–20 [24], and 1.6–17.0 [25]. However, in some other studies, the estimated R_0 ranged from 1.16 to 1.86 for p-H1N1 [2,26]. The discrepancy in R_0 compared to other epidemiological studies may due to the enlargement of disease transmission in indoor enclosures

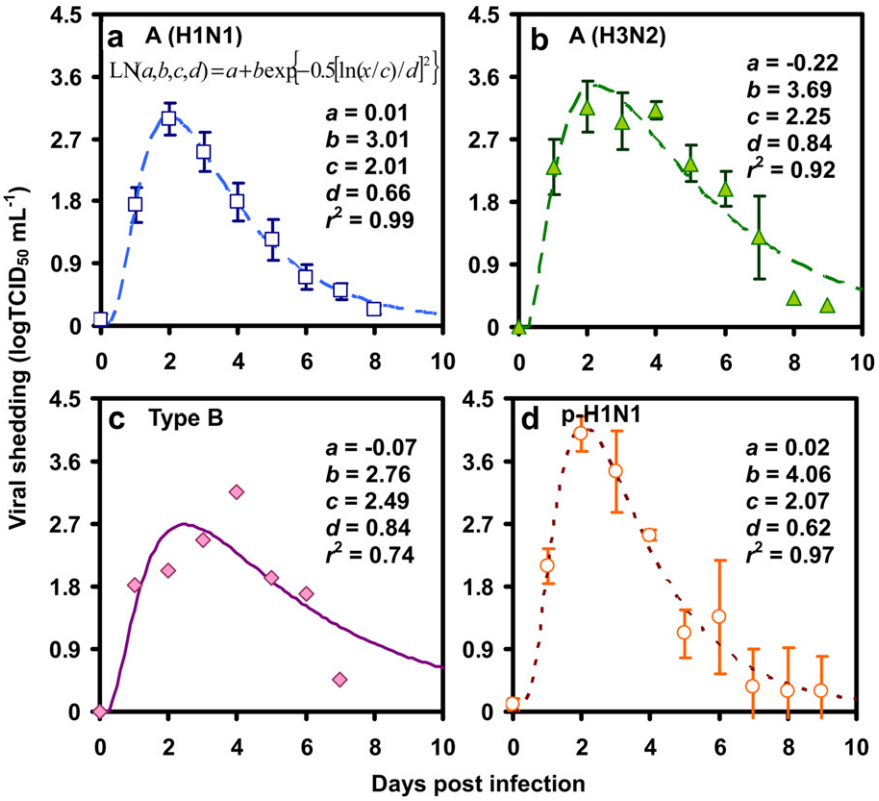

Fig. 3. 4-Parameter lognormal fitting curve best described the days post infection-specific viral shedding data for (a) A (H1N1) (b) A (H3N2) (c) Type B, and (d) p-H1N1, respectively.

where susceptibles and infectors gather with continuous aerosolized influenza exposure.

Fraser et al. [10] indicated that the timing of the onset of infectiousness relative to the onset of detectable clinical signs can be used to define the success of disease control strategies. The key variable is θ. The means and distributions of incubation, latent, and infectious periods are key determinants of θ. Here we have successfully estimated θ values for A (H1N1), A (H3N2), B, and p-H1N1. Yet, the value of θ may also depend on the joint distributions of latent and incubation periods. The value of θ for human influenza has been reported as 0.3–0.5 [10], yet several studies have suggested that it could be much lower based on the observations [27]. Therefore, the experimental and/or epidemiological studies of virus transmission in natural hosts designed to quantify transmission rates at different times after exposure are required. We suggested that there is a need for more robust empirical evidence on relationships between clinical evidence and infectiousness to enhance control measure strategies based on the present indoor R_0-θ control model.

4.2. Viral shedding data and risk estimates

For seasonal influenza, the mean duration of viral shedding was 4–5 days [19], whereas for p-H1N1, the mean duration of viral shedding ranged from 4 to 7 days [28]. The longer viral shedding duration of p-H1N1 reflected the larger potential in disease transmission and severity in comparison with seasonal influenza. Moreover, the estimated median infection risk of p-H1N1 was nearly 2–3 times higher than that of seasonal influenza ranging from 0.007 to 0.009, reflecting the higher infectiousness and transmissibility. However, this may due in part to in the non-pandemic period in which only a minority of patients infected by seasonal influenza virus attend to hospital service. As a result, the infection risk of p-H1N1 may be overestimated.

4.3. Model limitations

We estimated uncertainties based on a combination of quantitative methods. To consider uncertainties of certain parameters,

Table 1
Epidemiology parameter estimates of seasonal influenza and pandemic H1N1 2009.

Epidemiology parameters estimate	A (H1N1)	A (H3N2)	Type B	p-H1N1
Infection risk, P[a]	LN(0.009, 2.11)[b]	LN(0.007, 2.03)	LN(0.007, 2.57)	LN(0.020, 1.46)
Quantum generation rate, q (quanta d^{-1})[c]	LN(220, 2.33)	LN(159, 2.27)	LN(159, 2.78)	LN(478, 1.76)
Basic reproduction number, R_0[c]	LN(1.51, 2.54)	LN(1.10, 2.49)	LN(1.09, 2.99)	LN(3.20, 1.99)
Generation time, T_g (d)[d]	LN(3.16, 1.06)	LN(4.15, 1.04)	LN(3.62, 1.01)	LN(3.54, 1.06)
Asymptomatic infectious proportion, θ (%)[e]	LN(32, 1.35)	LN(23, 1.09)	LN(19, 1.07)	LN(22, 1.66)

[a] P = ILI positive proportion/Admission proportion, calculated based on database of Taiwan Centers for Disease Control (Taiwan CDC) and statistics of Taiwan Department of Health (Taiwan DOH).

[b] LN(gm, gsd): lognormal distribution with geometric mean (gm) and geometric standard deviation (gsd).

[c] See Table S2 in Supplementary materials.

[d] $T_g = \int_0^\infty tV(t)dt / \int_0^\infty V(t)dt$.

[e] θ = (Incubation period − Latent period)/Mean duration of viral shedding (see Table S3 in Supplementary materials).

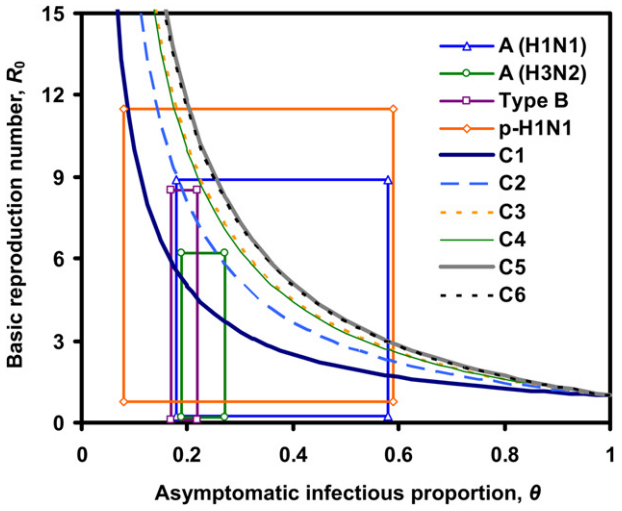

Fig. 4. R_0-θ critical control curves constructed based on potential combinations of control measures (C1 – C6, see Table S4 in Additional file 2) together with the rectangles indicated the impacts of control measures. The rectangles were delineated by 95% CIs of R_0 and θ estimates of A (H1N1), A (H3N2), type B, and p-H1N1, respectively. The rectangle with triangle, circle, square, and diamond represent A (H1N1), A (H3N2), type B, and p-H1N1, respectively.

lognormal model was presumed to obtain non-negative estimates, however, in real situation, it may not be the case. There are critical data gaps that affected both the results presented here and our ability to report and verify changes in airborne influenza virus droplets indoors. An integration of computational and mechanistic model would be helpful to understand the airflow pattern, size-specific droplet transmission modes indoors, and infectivity due to source proximity [14].

Data are substantially lacking for quantum generation rate of infected individuals. Key parameters including classroom volume, susceptibles and infectors in the classroom, and ventilation rate would greatly influence the disease severity and transmission.

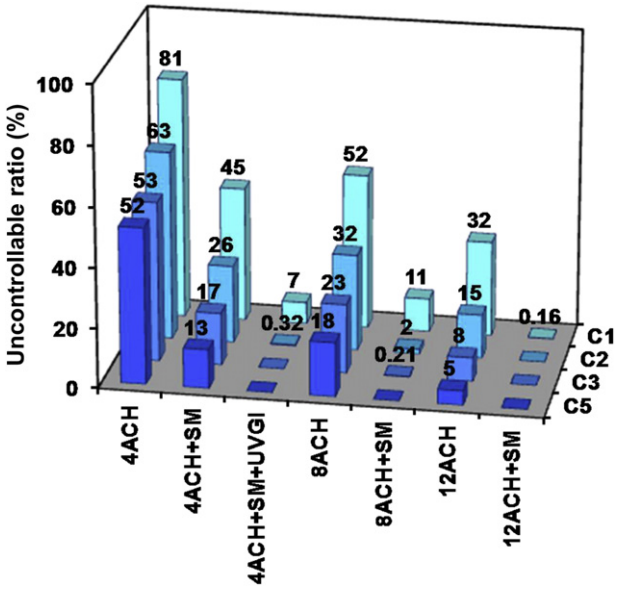

Fig. 5. Potentials of p-H1N1 outbreak containment assessed by applying both non-engineering (C1, C2, C3, and C5) and engineering (EV, SM, UVGI, and HEPA) controls with different combinations. Where UVGI could be replaced by HEPA and implementing C5 together with EV, SM, and UVGI reveal complete outbreak control.

Specifically, high-efficiency ventilation could rapidly remove infectious pathogens and decrease infection risks, however, it is hard to achieve realistically; given the same outdoor air supply rate, larger airspace volume would reduce q and R_0 due to ventilation dilution effect; more susceptibles and infectors gathering in the airspace could result in higher infection risk as well as faster and more serious disease transmission because of more frequent and complex contact structures, host moving patterns, and greater virus spread. These factors affect significantly the control measure efficiencies, especially for engineering interventions. However, there is a lack of measurement data of dominant coefficients describing droplet size-specific shedding distribution, environmental process factors, host–environment interactions, and exposure dose–response relationships [29].

In this study, quantum generation rates were estimated by the Wells-Riley mathematical equation under well-mixed and steady-state conditions. Premises of well-mixed and steady-state would probably give rise to either underestimation or overestimation of disease severity due to various spatial distributions and proximity to the infectious source. Alternatively, a transient Wells-Riley equation may be applied to consider exposures occurring at multiple time periods whenever there is integrated account of the staying time, the time pathogen being expired, the exact ventilation schedule, the more precise contact situation, etc [30]. Based on current estimation process, whether a super-spreader exists in the indoor environment is hardly recognized, however, given a precise location and detection of an infector, engineering control measures such as UVGI and HEPA could be implemented more efficiently as to eliminate the infectious source at first time. Although massive application of UVGI and HEPA filter may not be feasible realistically, this study suggested that these equipments could be implemented in high population density locations such as school classroom [22,31,32]. The Wells-Riley equation is basically applied in a confined airspace, detailed surveillance of demography and epidemiology would help understanding the transmissions in the bus, between classes or within communities [30], yet based on well-mixed and steady-state conditions as well.

While building up a control measure model, similar assumption was made that people in the community or indoor environments mix homogeneously. Besides, the distribution of the time to symptoms is assumed to be exponential. Nevertheless, in real situation, influenza aerosols are not homogeneously spatially distributed partly due to ventilation, gravitational settling, and virus inactivation, and the generated influenza concentrations are varied depending on the position where the index patient emitting virus particles and the location of virus particles formation. Influenza virus could enter into the airspace through an infected person by breathing, talking, coughing, and sneezing [33,34]. Further tracking in influenza airflow and quantification in virus concentration after emission is needed to estimate infection risks more precisely.

There are four possible exposure routes for influenza: (i) contact, (ii) inhalation, (iii) inspiration, and (iv) direct spray which can be categorized mainly based on their aerodynamic diameters. Nicas and Jones [35] suggested that the hand contact and droplet spray were two dominant routes leading to risk of infection based on various scenarios. Atkinson and Wein [36] concluded that respirable particle inhalation was the dominant exposure route. However, the interactions and transforming mechanisms among four exposure pathways are still vague and controversial and thus worth further studying.

4.4. Implications for indoor environment setting

Numerous factors were found to affect the infectivity of influenza viruses such as temperature, humidity, ultraviolet radiation

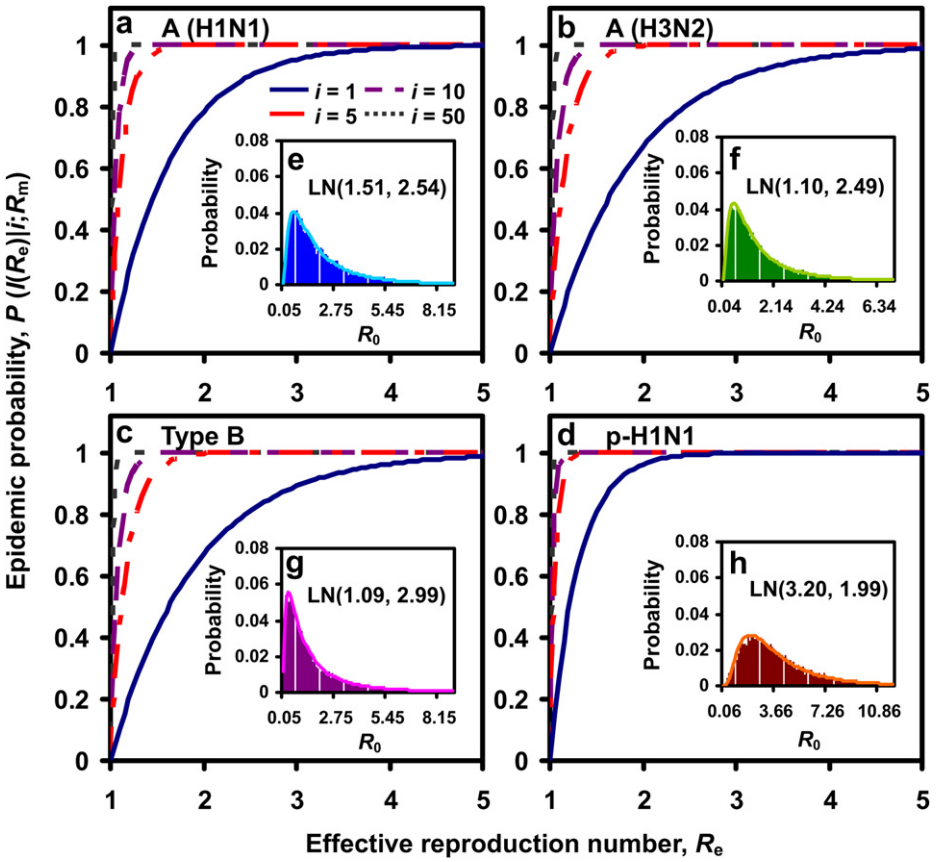

Fig. 6. Indoor epidemic probability of an outbreak of (a) A (H1N1), (b) A (H3N2), (c) Type B, and (d) p-H1N1 in a susceptible population based on a single, 5, 10, and 50 infectious cases introduction. (e), (f), (g), and (h) show the R_0 distributions of A (H1N1), A (H3N2), type B, and p-H1N1, respectively.

[32], school schedules, and contact routes. Among these, humidity and temperature were demonstrated to be the leading factors in influenza infection in the indoor environment [37,38]. In the study that guinea pig as a model host, the authors indicated both cold (5 °C) and dry (relative humidity, RH: 20%) conditions favor transmission [37]. Yang and Marr [39] further evidenced the theory that maintaining high indoor relative humidity (90%) as well as ventilation may help reduce chances of influenza A virus infection. Therefore, based on experimental and simulated results, 20 °C together with 90% RH is suggested in indoor environment to enhance prevention of influenza infection.

This study provided an integrated approach to assess influenza transmission indoors and control measure efficiencies through considering the combinative measures of non-engineering and engineering control in an elementary school classroom. For seasonal influenza, optimal control efficiency can be achieved by considering only the non-engineering control strategies, whereas for p-H1N1, additional implementation of engineering control measures reveals efficiently outbreak containment even low EV (4 ACH) was considered (Fig. 5). Non-engineering control measure combination (C5) together with EV(12ACH), SM, UVGI, and HEPA displayed excellent disease containment potential that may be applicable whenever there is a super-spreader or during pandemics.

To better contain influenza transmission and reduce infection, a model regarding the relationship among influenza virus, host, and indoor environment can be constructed to describe the complex dynamics of environmental processes and to achieve optimal indoor control measures [29]. Moreover, a better understanding of the role of human behavior in optimal environmental influenza interventions and mechanisms responsible for virus transmission is critical for predicting airborne infectious virus changes and guiding the design and implementation of control policies.

5. Conclusions

In this study, an indoor transmission model was used to assess influenza transmission risk along with the estimations of epidemiology parameters based on human experimental data. The proposed control strategies combined with non-engineering and engineering interventions could completely control p-H1N1 outbreak. A general form of multi-control measure model developed here could be further implemented in more complicated infectious circumstances. The proposed mathematical model for assessing the probability of epidemic provide a general picture of how the alteration in introduced infected would affect the disease epidemic under certain effective reproduction number. Our study can be incorporated into the relationship among influenza virus, host, and indoor environment for better understanding the complex dynamics of environmental processes and to achieve optimal indoor control measures.

Acknowledgments

The authors acknowledge the financial support of the National Science Council of Republic of China under Grant NSC 100-2313-B-002-012-MY3.

Appendix A. Supplementary data

Supplementary data related to this article can be found online at http://dx.doi.org/10.1016/j.buildenv.2013.01.014.

References

[1] WHO (World Health Organization). Global alert and response (GAR): influenza updates, http://www.who.int/csr/disease/influenza/2011_02_25_GIP_surveillance/en/index.html; 25 February 2011 [accessed on March 2011].
[2] Yang Y, Sugimoto JD, Halloran ME, Basta NE, Chao DL, Matrajt L, et al. The transmissibility and control of pandemic influenza A (H1N1) virus. Science 2009;326:729–33.
[3] WHO (World Health Organization). Global alert and response (GAR): WHO recommendations for the post-pandemic period, http://www.who.int/csr/disease/swineflu/notes/briefing_20100810/en/index.html [accessed on August 2012].
[4] Schrauwen EJA, Herfst S, Chutinimitkul S, Bestebroer TM, Rimmelzwaan GF, Osterhaus ADME, et al. Possible increased pathogenicity of pandemic (H1N1) 2009 influenza virus upon reassortment. Emerg Infect Dis 2011;17:200–8.
[5] Chowell G, Bertozzi SM, Colchero MA, Lopez-Gatell H, Alpuche-Aranda C, Hernandez M, et al. Severe respiratory disease concurrent with the circulation of H1N1 influenza. N Engl J Med 2009;361:674–9.
[6] Ngaosuwankul N, Noisumdaeng P, Komolsiri P, Pooruk P, Chokephaibulkit K, Chotpitayasunondh T, et al. Influenza A viral loads in respiratory samples collected from patients infected with pandemic H1N1, seasonal H1N1 and H3N2 viruses. Virol J 2010;7:75.
[7] Cowling BJ, Chan KH, Fang VJ, Lau LLH, So HC, Fung ROP, et al. Comparative epidemiology of pandemic and seasonal influenza A in households. N Engl J Med 2010;362:2175–84.
[8] Sugimoto JD, Borse NN, Ta ML, Stockman LJ, Fischer GE, Yang Y, et al. The effect of age on transmission of 2009 pandemic influenza A (H1N1) in a camp and associated households. Epidemiology 2011;22:180–7.
[9] Jefferson T, del Mar C, Dooley L, Ferroni E, Al-Ansary LA, Bawazeer GA, et al. Physical interventions to interrupt or reduce the spread of respiratory viruses: systemic review. Br Med J 2009;339:b3675.
[10] Fraser C, Riley S, Anderson RM, Ferguson NM. Factors that make an infectious disease outbreak controllable. Proc Natl Acad Sci U S A 2004;101:6146–51.
[11] Bolashikov ZD, Melikov AK. Methods for air cleaning and protection of building occupants from airborne pathogens. Build Environ 2009;44:1378–85.
[12] Lim T, Cho J, Kim BS. Predictions and measurements of the stack effect on indoor airborne virus transmission in a high-rise hospital building. Build Environ 2011;46:2413–24.
[13] Zuraimi MS, Nilsson GJ, Magee RJ. Removing indoor particles using portable air cleaners: implications for residential infection transmission. Build Environ 2011;46:2512–9.
[14] Zhu S, Srebic J, Spengler JD, Demokritou P. An advanced numerical model for the assessment of airborne transmission of influenza in bus microenvironments. Build Environ 2012;47:67–75.
[15] Anderson RM, May RM. Infectious diseases of humans: dynamics and control. Oxford: Oxford University Press; 1991.
[16] Taiwan CDC. (Centers for Disease Control, R.O.C. (Taiwan)). Practical guideline for prevention and control of seasonal influenza [accessed on December 2012], http://flu.cdc.gov.tw/public/Attachment/211161638509.pdf.
[17] Chuang JH, Huang AS, Huang WT, Liu MT, Chou JH, Chang FY, et al. National surveillance of influenza during the pandemic (2009–10) and post-pandemic (2010–11) periods in Taiwan. PLoS ONE 2012;7:e36120.
[18] Rudnick SN, Milton DK. Risk of indoor airborne infection transmission estimated from carbon dioxide concentration. Indoor Air 2003;13:237–45.
[19] Carrat F, Vergu E, Ferguson NM, Lemaitre M, Cauchemez S, Leach S, et al. Time lines of infection and disease in human influenza: a review of volunteer challenge studies. Am J Epidemiol 2008;167:775–85.
[20] Liao CM, Chen SC, Chang CF. Modeling respiratory infection control measure effects. Epidemiol Infect 2008;136:299–308.
[21] Taylor HM, Karlin S. An introduction to stochastic modeling. San Diego: Academic Press; 1994.
[22] Chen SC, Chang CF, Liao CM. Predictive models of control strategies involved in containing indoor airborne infections. Indoor Air 2006;16:469–81.
[23] Chen SC, Liao CM. Modelling control measures to reduce the impact of pandemic influenza among schoolchildren. Epidemiol Infect 2008;136:1035–45.
[24] Rvachev LA, Longini IM. A mathematical-model for the global spread of influenza. Math Biosci 1985;75:3–23.
[25] Vynnycky E, Trindall A, Mangtani P. Estimates of the reproduction numbers of Spanish influenza using morbidity data. Int J Epidemiol 2007;36:881–9.
[26] Paine S, Mercer GN, Kelly PM, Bandaranayake D, Baker MG, Huang QS, et al. Transmissibility of 2009 pandemic influenza A(H1N1) in New Zealand: effective reproduction number and influence of age, ethnicity and importations. Euro Surveill 2010;15:19591.
[27] Yamagishi T, Matsui T, Nakamura N, Oyama T, Taniguchi K, Aoki T, et al. Onset and duration of symptoms and timing of disease transmission of 2009 influenza A (H1N1) in an outbreak in Fukuoka, Japan, June 2009. Jpn J Infect Dis 2010;63:327–31.
[28] Li CC, Wang L, Eng HL, You HL, Chang LS, Tang KS, et al. Correlation of pandemic (H1N1) 2009 viral load with disease severity and prolonged viral shedding in children. Emerg Infect Dis 2010;16:1265–72.
[29] Spicknall IH, Koopman JS, Nicas M, Pujol JM, Li S, Eisenberg JNS. Informing optimal environmental influenza interventions: how the host, agent, and environment alter dominant routes of transmission. PLoS Comput Biol 2010;6:e1000969.
[30] Gao X, Li Y, Leung GM. Ventilation control of indoor transmission of airborne disease in an urban community. Indoor Built Environ 2009;18:205–18.
[31] Brickner PW, Vincent RL, First M, Nardell E, Murray M, Kaufman W. The application of ultraviolet germicidal irradiation to control transmission of airborne disease: bioterrorism countermeasure. Public Health Rep 2003;118:99–114.
[32] Kowalski W. Ultraviolet germicidal irradiation handbook: UVGI for air and surface disinfection. New York: Springer Verlag; 2009.
[33] Stelzer-Braid S, Oliver BG, Blazey AJ, Argent E, Newsome TP, Rawlinson WD, et al. Exhalation of respiratory viruses by breathing, coughing, and talking. J Med Virol 2009;81:1674–9.
[34] Gupta JK, Lin CH, Chen QY. Transport of expiratory droplets in an aircraft cabin. Indoor Air 2011;21:3–11.
[35] Nicas M, Jones RM. Relative contributions of four exposure pathways to influenza infection risk. Risk Anal 2009;29:1292–303.
[36] Atkinson MP, Wein LM. Quantifying the routes of transmission for pandemic influenza. Bull Math Biol 2008;70:820–67.
[37] Lowen AC, Mubareka S, Steel J, Palese P. Influenza virus transmission is dependent on relative humidity and temperature. PLoS Pathog 2007;3:1470–6.
[38] Steel J, Palese P, Lowen AC. Transmission of a 2009 pandemic influenza virus shows a sensitivity to temperature and humidity similar to that of an H3N2 seasonal strain. J Virol 2011;85:1400–2.
[39] Yang W, Marr LC. Dynamics of airborne influenza A viruses indoors and dependence on humidity. PLoS ONE 2011;6:e21481.